**EUROPEAN ORGANIZATION FOR NUCLEAR RESEARCH**
**European Laboratory for Particle Physics**

**[Institute]**

[Institute address]

**Internal Note/**
ALICE reference number
ALICE-INT-2004-009 version 1.0
Institute reference number
[-]
Date of last change
2004-03-10

# Probes and Observables
# PPR Chapter 6.8

**Authors:**

J. Bartke, P. A. Bolokhov, M. A. Braun, G. A. Feofilov, M. Gazdzicki, V. Koch, V. P. Kondriatev, A. Leonidov, St. Mrowczynski, G. Paic, W. Retyk, G. Wilk, V. V. Vechernin

**Abstract:**

The main motivation for a broad experimental programme of nucleus-nucleus (A-A) collisions at high energies (AGS, SPS and RHIC) is the search for the phase transition to the Quark Gluon Plasma (QGP) [1]. Currently [2] the theoretical calculations indicate that a way to infer the nature and order of this transition is to look for the fluctuations in different parameters measured not as a value averaged over many events like slopes of momentum spectra, multiplicity, mean value of momentum etc but rather for each event, and comparing the excursion of these values compared with the average behaviour. We call then this approach **event-by-event physics**. It also is expected that the measured fluctuations will give us information about the degree of thermalization one achieves in heavy-ion collisions, comparing the evolution of the nonstatistical fluctuations with centrality. The challenge of this type of studies is that, beyond fluctuations linked to the details of the phase transition, there are number of other fluctuations which may appear. They impact different observables and act on different scales. As an example let us mention two of them. Quantum number, and energy and momentum conservation laws correlate all particles in the collision and thus influence fluctuations at large scales. On the other hand, short-range correlations due to quantum statistics obeyed by fermions and bosons result in suppression (fermions) or enhancement (bosons) of fluctuations at small scales.

Contact person: M.Gazdzicki

# Contents

# Probes and Observables

## 6.8 Event-by-event physics

Editor: Marek Gazdzicki. Contributors: W. Retyk, P. A. Bolokhov, M. A. Braun, G. A. Feofilov, V. P. Kondriatev, V. V. Vechernin, V. Koch, St. Mrówczyński, G. Wilk, J. Bartke

### 6.8.1 Introduction

The main motivation for a broad experimental programme of nucleus-nucleus (A-A) collisions at high energies (AGS, SPS and RHIC) is the search for the phase transition to the Quark Gluon Plasma (QGP) [1]. Currently [2] the theoretical calculations indicate that a way to infer the nature and order of this transition is to look for the fluctuations in different parameters measured not as a value averaged over many events like slopes of momentum spectra, multiplicity, mean value of momentum etc but rather for each event, and comparing the excursion of these values compared with the average behaviour. We call then this approach **event-by-event physics**. It also is expected that the measured fluctuations will give us information about the degree of thermalization one achieves in heavy-ion collisions, comparing the evolution of the nonstatistical fluctuations with centrality. The challenge of this type of studies is that, beyond fluctuations linked to the details of the phase transition, there are number of other fluctuations which may appear. They impact different observables and act on different scales. As an example let us mention two of them. Quantum number, and energy and momentum conservation laws correlate all particles in the collision and thus influence fluctuations at large scales. On the other hand, short-range correlations due to quantum statistics obeyed by fermions and bosons result in suppression (fermions) or enhancement (bosons) of fluctuations at small scales.

The rapid development of the event-by-event physics in recent years is directly related to the experimental progress in the field of high-energy nucleus-nucleus collisions. Recent detector technologies and collision energies allow the detection of a large fraction of thousands of hadrons produced in each central Pb+Pb collision at SPS, RHIC and LHC energies. This high statistics of particles registered for a single event allows for a precise estimate of various event characteristics.

Active study of event-by-event fluctuations in A+A collisions was initiated by the NA49 experiment [3, 4] at the CERN SPS. The experimental setup is based on four large-acceptance TPCs which yield high momentum and two-track resolution data on identified hadron production. More than $10^3$ hadrons are measured in a single central PbPb collision at the SPS and the typical number of registered events is $10^6$. Event-by-event fluctuations of charged particle multiplicity, strangeness production, electric charge and transverse momentum are the focus of this study. A similar strategy was adopted by the STAR experiment at RHIC and will also be followed by ALICE at the LHC. First results on event-by-event fluctuations in nuclear collisions at the SPS and RHIC are now available. The experimental procedures, statistical tools, and theoretical models are challenged by the requirements of event-by-event study.

So far the results of the SPS and RHIC experiments and their theoretical interpretation have allowed us to establish neither clear fluctuation patterns nor satisfactory projections to higher energies. Therefore the scope of this section is limited to a review of the SPS and RHIC results and to a presentation of the possible event-by-event observables at the LHC.

### 6.8.2 Present status of event-by-event fluctuations at the SPS and RHIC

The present results at the SPS and RHIC indicate that statistical models of strong interactions reproduce surprisingly well the energy dependence of entropy and strangeness production [5] and the hadronization process [6], resulting in a correct description of hadron yield systematics (see section 6.2). However, the interpretation of the data within statistical models is under discussion. These models are not commonly recognized as valid tools to investigate high-energy nuclear collisions. Indeed, their basic assumptions cannot be derived from the commonly accepted theory of strong interactions QCD. On the other hand it is difficult to apply QCD for the interpretation of the experimental results since almost all effects connected to the transition to QGP are in the domain of soft processes for which experimentally testable

predictions of QCD are not available. Attempts to build phenomenological, QCD-inspired, models have not been very successful [7] either. Conclusive interpretation of the data within these models seems to be impossible since one cannot estimate the uncertainties due to the approximations introduced.

Thus, the questions concerning interpretation of A-A results unavoidably lead to the more fundamental questions about our understanding of strong interactions and the validity of various frameworks. In particular, further tests of the limits of applicability of statistical models are urgently needed. Within this context the study of event-by-event fluctuations [8, 9] plays a special role as it allows for independent tests of competing approaches.

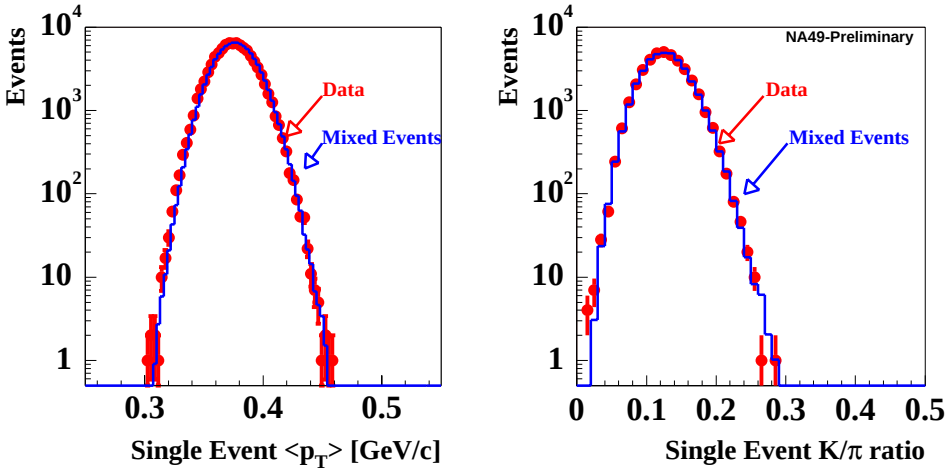


**Figure 6.1:** The event-by-event fluctuations of the mean transverse momentum and the kaon-to-pion ratio for central Pb+Pb collisions at 158 A·GeV as measured by NA49. The solid lines indicate fluctuations calculated assuming independent particle emission (the 'mixed' event procedure).

The first results on fluctuations in central Pb+Pb collisions at 158 A·GeV, measured in the forward rapidity region, indicate that fluctuations of transverse momentum $p_T$ [8] and kaon-to-pion ratio [9] are small, see Fig. 6.1. They are close to the fluctuations expected in the case of uncorrelated particle production (statistical fluctuations), and thus consistent with the expectation derived within statistical models [10] when the small effects due to quantum statistics, Coulomb interaction, and resonance decays are taken into account.

Systematic, quantitative study of event-by-event fluctuations is done using the $\Phi$ measure of fluctuations [11] or closely related measures [12]. The $\Phi$ measure is defined as follows. One introduces a single-particle variable $z \stackrel{\text{def}}{=} x - \overline{x}$ with the over-line denoting average over a single particle inclusive distribution. Here, we identify $x$ with $p_T$. The event variable $Z$, which is a multi-particle analogue of $z$, is defined as $Z \stackrel{\text{def}}{=} \sum_{i=1}^{N}(x_i - \overline{x})$, where the summation runs over particles from a given event. Finally, the $\Phi$ measure is defined as

$$\Phi \stackrel{\text{def}}{=} \sqrt{\frac{\langle Z^2 \rangle}{\langle N \rangle}} - \sqrt{\overline{z^2}}\,.$$

It allows us to remove the influence of 'unwanted' volume fluctuations (due to variations in the impact parameter of the collision resulting in turn in variations in the number of nucleons participating in the collision). The values of $\Phi_{p_T}$ (the measuere of transverse momentum fluctuations) obtained for all inelastic

p+p interactions and nucleus–nucleus (from C+C to central Pb+Pb) collisions at 158 A·GeV are shown in Fig. 6.2 as a function of the mean number of participant nucleons [13] at forward rapidities (4–5.5). We note that the value of $\Phi_{P_T}$ for uncorrelated particle production is equal to zero. The results indicate a significant non-statistical fluctuations of transverse momentum for light nuclei and peripheral Pb+Pb collisions. Similar results have been reported by PHENIX at RHIC [14]. The interpretation of these interesting results is under discussion [15–17]. For central Pb+Pb (Au+Au) collisions significant non-statistical $p_T$ fluctuations are reported at midrapidity by STAR at RHIC [18] and CERES at SPS [19]. The origin of these fluctuations is still unclear.

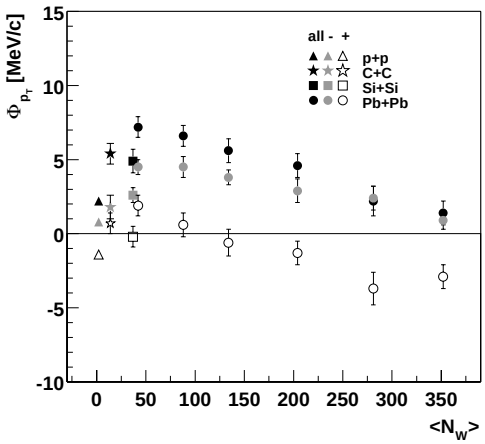


**Figure 6.2:** The $\Phi_{p_T}$ fluctuation measure dependence on the number of participant nucleons for nucleus–nucleus collisions and all inelastic p+p interactions at 158 A·GeV.

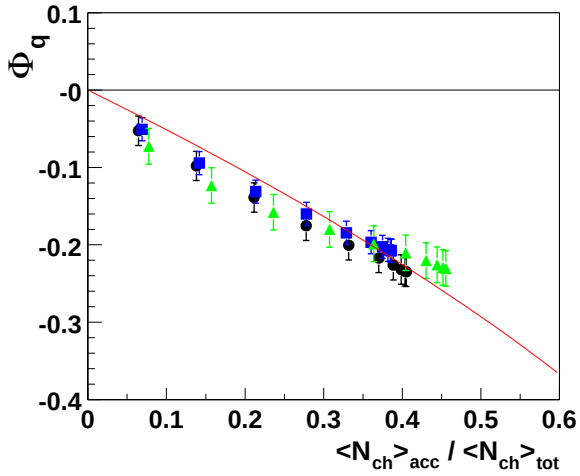


**Figure 6.3:** The $\Phi_q$ fluctuation measure for central Pb+Pb collisions at 40 (triangles), 80 (squares) and 158 (circles) A·GeV as a function of the fraction of accepted particles varied by changing the rapidity window. The inclined solid line indicates fluctuations expected only due to global charge conservation.

Recent suggestions [20, 21] that event-by-event fluctuations of electric charge in high-energy A-A collisions may provide information on the state of matter at the early stage of the collision triggered corresponding experimental studies. The first results [13, 22, 23] (see Fig. 6.3) indicate that the net electric charge fluctuations are governed by the conservation of electric charge [24,25] and that additional contributions, if any, are small.

Thus, the suppression of fluctuations predicted for the case of QGP creation is not observed. However, it have been suggested that processes following QGP hadronization like hadronic rescattering [26] and resonance decays [24] may almost completely wipe out fluctuations originally developed in the QGP phase.

The WA98 Collaboration searched for anomalous fluctuations of the ratio of neutral to charged pions predicted to occur in the case of creation of Disoriented Chiral Condensate (DCC). No signal was observed [27].

### 6.8.3 Event-by-event fluctuations in ALICE

There are numerous well-established (i.e. observed and identified in p+p and/or A-A interactions) physical sources of event-by-event fluctuations in high-energy nucleus-nucleus collisions:

- geometrical (impact parameter) fluctuations [11],
- motional and material conservation laws [24, 25],
- anisotropic flow [28],

- resonance and string decays [10, 24, 29],
- jets and minijets [16],
- quantum statistics [10],
- Coulomb interactions [10].

Many exotic (still not observed and/or identified) phenomena may also occur and significantly impact the observed fluctuations. Among them are:

- colour collective phenomena [30],
- frozen statistical QGP fluctuations [20, 21],
- temperature fluctuations [31],
- formation of colour ropes [17],
- creation of DCC [32],
- creation of strangelets [33].

Dedicated analysis methods and statistical tools are well established in order to study the majority of the standard processes listed above (geometrical fluctuations, quantum statistics, Coulomb interactions, resonance production, anisotropic flow). Their impact on event-by-event fluctuations can be therefore estimated based on the experimental results and thus they serve as a background above which other effects are looked for.

Of special interest at LHC energies is the study of jet and minijet production in nucleus–ucleus collisions. Since the jet/minijet production cross-section measured in p+p($\bar{\text{p}}$) interactions strongly increases with energy, one expects that copious jet/minijet production may be a dominant feature of A-A collisions at the LHC. Standard methods developed for the jet search in elementary interactions fail in the case of A-A collisions (at least for $E_T < 50$ GeV on account of the very high background of soft hadrons and other jets). Direct jet identification is possible only at very high $p_T$. On the other hand, the hadrons originating from a jet are correlated in momentum space and therefore jet production should lead to an increase of fluctuations. Consequently, the study of event-by-event fluctuations may yield important information on jet/minijet production not accessible by direct methods because of high background. Copious jet/minijet production and consequently large fluctuations may, however, shadow fluctuations caused by other processes of interest. It is therefore clear that the relation between jet/minijet production and searched for event-by-event fluctuations needs careful study.

In the following we shall discuss in more detail this and other selected subjects of event-by-event physics in relation to the ALICE experiment at the LHC.

#### 6.8.3.1 Jets and fluctuations

*i. $p_T$ fluctuations*

In this subsection we report results of simulations concerning the influence of jet production on event-by-event fluctuations of transverse momentum as measured by the ALICE TPC. In order to study exclusively the effect of jet production, a simple model of central Pb+Pb collisions at the LHC was developed. Two independent sources of particle production were assumed: the ‘soft’ component models production of particles at low transverse momenta, whereas the ‘hard’ component simulates particles originating from jets. The ‘soft’ component was simulated assuming independent production of charged

hadrons. The rapidity and azimuthal angle distributions were assumed to be uniform. The transverse momentum spectrum was generated according to a 'thermal' distribution:

$$\frac{1}{p_T}\frac{dn}{dp_T} = C \cdot \exp\left(-\frac{m_T}{T}\right), \tag{6.1}$$

where $T = 190$ MeV is an inverse slope parameter, and $C$ is an arbitrary normalization parameter. The rapidity density distribution of the 'soft' component was taken to be Gaussian with a mean of 6000 and $\sigma = 1000$. For each event, in addition to 'soft' component, a 'hard' component modelling jet production was generated. The $p_T$ spectrum of jets produced in central PbPb collisions at 5.5 TeV/(N+N) was calculated by scaling the corresponding $p_T$ spectrum obtained for p+p interactions at 5.5 TeV using PYTHIA (version 6.1) with the standard (2 jet-events, LO calculations and no initial and no final state radiation) parameters. The scaling factor for the spectrum normalized to mean multiplicity was calculated following the pQCD-based rule $\langle jet \rangle \sim \langle N_W \rangle^{4/3}$, where $\langle N_W \rangle$ is the mean number of wounded nucleons.

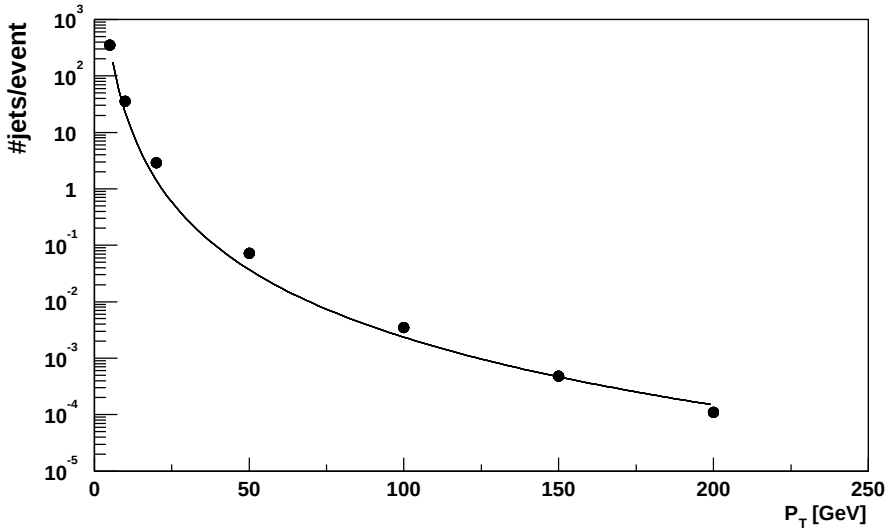


**Figure 6.4:** Transverse momentum spectrum of jets in central Pb+Pb collisions at 5.5 TeV/(N+N) assumed in the simulation.

The resulting jet $p_T$-spectrum is presented in Fig. 6.4. The multiplicity distribution of jets was assumed to be Poissonian. The jet fragmentation properties were introduced by a parametrization of the appropriate distributions generated again within PYTHIA.

Events generated according to the model within the ALIROOT framework were passed through the ALICE TPC fast simulation chain, which allowed for a proper introduction of the detector acceptances. For the final analysis of fluctuations, only tracks measurable (long enough for reconstruction) in the ALICE TPC were selected and the $\Phi_{p_T}$ fluctuation measure was calculated for them.

The observed transverse momentum fluctuations depend on the acceptance selected for the study. In order to investigate this effect we introduced a rectangular acceptance window defined in azimuthal angle $\psi$ and pseudo-rapidity $\eta$, in addition to the geometrical TPC acceptance. The size of the window

$$L_{\eta,\psi} = \sqrt{\Delta\eta^2 + \Delta\psi^2} \tag{6.2}$$

was varied by scaling $\Delta\eta$ and $\Delta\psi$ by the same factor. In this procedure we assumed that $\Delta\eta/\Delta\psi = 2/(2\cdot\pi) \approx 0.32$.

The dependence of $\Phi_{p_T}$ on $L_{\eta,\psi}$ is shown in Fig. 6.5 for two cases: 'soft' component only and 'soft' + 'hard' components, as defined above. In the case of the 'soft' component, independently of the size

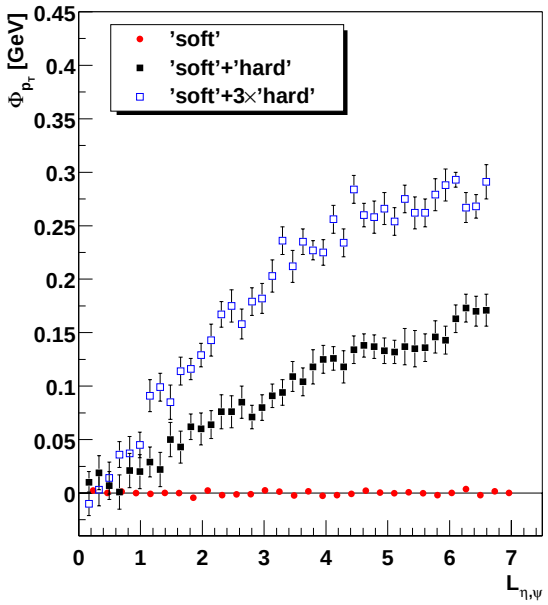


**Figure 6.5:** The dependence of $\Phi_{p_T}$ on the acceptance for 'soft' component (dots), 'hard' + 'soft' components (squares) and the contribution of hard component increased by a factor of 3 (open squares).

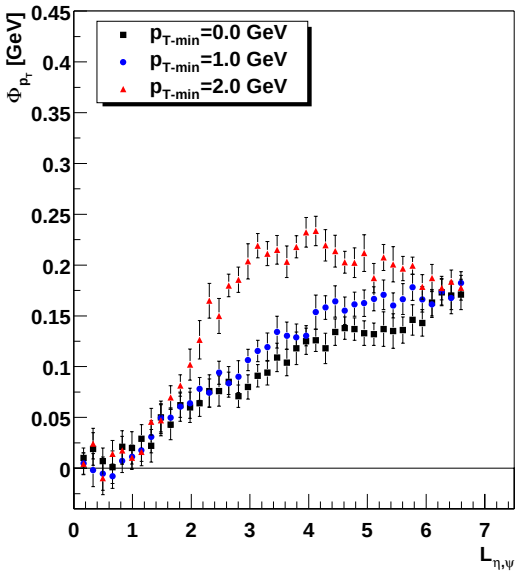


**Figure 6.6:** The dependence of $\Phi_{p_T}$ on the acceptance for 'hard' + 'soft' component model without (squares) and with low $p_T$ cut at 1.0 GeV/c (blue dots) or 2.0 GeV/c (triangles).

of the acceptance window, the value of $\Phi_{p_T}$ was equal to zero. This result was expected because of the assumption of uncorrelated particle production in the 'soft' component model. However, in the 'soft'+ 'hard' case large non-zero values of $\Phi_{p_T}$ were obtained. The strong event-by-event fluctuations result from the correlated particle production in the 'hard' component. The $\Phi_{p_T}$ increases with the size of the acceptance window $L_{\eta,\psi}$. In order to understand this dependence it is useful to consider two asymptotic regions. For very small acceptance ($L_{\eta,\psi} \to 0$) at most one particle from a jet is accepted and thus the correlation of particles within a jet is not seen, $\Phi_{p_T} \to 0$. For very large acceptances all particles from a jet are accepted and a positive value of $\Phi_{p_T}$ is measured. With increasing acceptance one increases proportionally the number of accepted jet- and 'soft'- hadrons. In this limiting case the value of $\Phi_{p_T}$ should be independent of the acceptance because of the 'intensive' property of the $\Phi$ measure. The expected saturation of $\Phi_{p_T}$ for large acceptance is, however, not observed in Fig. 6.5. This is because the ALICE TPC acceptance in pseudo-rapidity is too small. Finally, in order to illustrate the sensitivity of the $p_T$ fluctuations on the ratio between 'hard' and 'soft' components we increased the expected jet multiplicity by a factor of 3; the results are shown in Fig. 6.5. by open symbols.

Since the fraction of particles originating from the 'hard' component increases with increasing $p_T$, one expects an increase of $\Phi_{p_T}$ when a low $p_T$ cut is applied to select particles for the analysis. In fact this is observed in Fig. 6.6 where the results without $p_T$ cut (squares) and after a low $p_T$ cut at 1.0 GeV/c (dots) and 2.0 GeV/c (triangles) are plotted. The results for a 2 GeV/c cut suggest an early onset of saturation of $\Phi_{p_T}$ with $L_{\eta,\psi}$ which may be due to the narrowing of the jet extension in $L_{\eta,\psi}$ after increasing the low $p_T$ cut.

In the previous study only the geometrical acceptance of ALICE TPC was taken into account. In the following the influence of detection inefficiency is discussed. First we consider the effect of random track losses due to tracking and fitting problems. In Fig. 6.7 the standard results obtained assuming a perfect detection and the result that includes random losses of 10% are compared. The difference is small in comparison to the expected effect due to the presence of jets. Then we simulate losses of tracks that

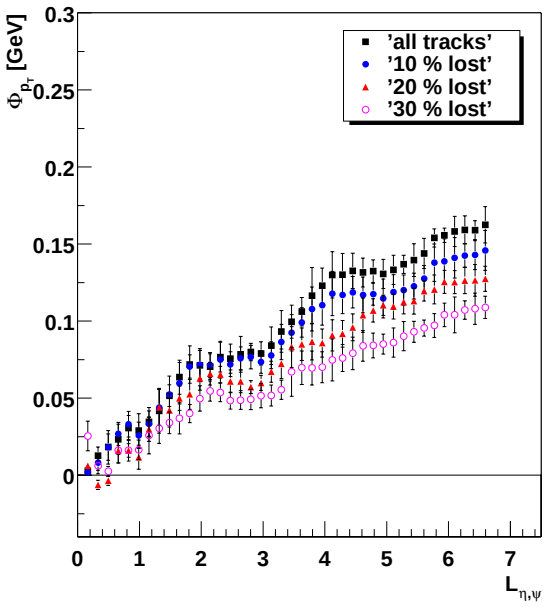


**Figure 6.7:** The dependence of $\Phi_{p_T}$ on the acceptance for 'hard' + 'soft' component model including possible effect of random track losses due to reconstruction inefficiency.

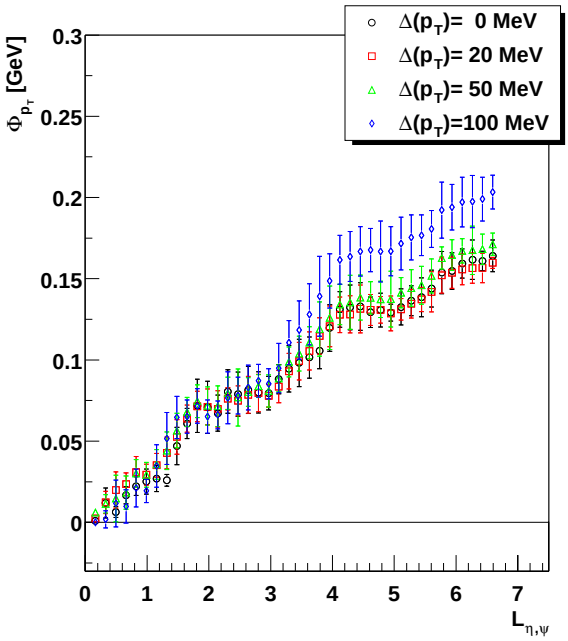


**Figure 6.8:** The dependence of $\Phi_{p_T}$ on the acceptance for 'hard' + 'soft' component model including possible effect of limited two track resolution modeled by lower cut on transverse momentum difference of two tracks.

are close in the detector space (effect of the two-track resolution). We assume that tracks that have a neighbour track with $\Delta p_T = |p_{T1} - p_{T2}| < cut$ MeV/c are lost. The results obtained including the effect of two-track resolution are shown in Fig. 6.8. The bias is small in comparison to the expected effect due to presence of jets.

In conclusion, the expected jet production in central Pb+Pb collisions at 5.5 TeV/(N+N) should lead to large event-by-event fluctuations of transverse momentum. This may allow one to test various models of jet production in the jet $p_T$ region not accessible for the standard methods of jet detection. On the other hand, fluctuations due to jet production should be taken into account when considering the detection of fluctuations due to other processes.

The influence of random detection inefficiencies as well as two-track resolution was estimated to be small for $p_T$ fluctuations as expected for unquenched jet production.

*ii. Fluctuations of transverse energy flow*

In this subsection we discuss an event-by-event azimuthal asymmetry in the transverse energy flow induced by the minijet dynamics [34]. The underlying idea is that the presence of new physics brought in by semihard degrees of freedom should manifest itself through reasonably well-defined changes in the inelasticity pattern that can (we hope) be measured experimentally, depending on the relative weight of minijet and soft hadronic contributions to the inelastic cross-section. Let us stress, that in order to reproduce an experimentally observed transverse energy spectrum, the description of minijet dynamics should go beyond the lowest-order two-to-two elastic scattering and include, in particular, initial and final state radiation (see for example Ref. [35]) as included into the HIJING Monte Carlo event generator [36]. HIJING allows one to study the effects due to the presence of semihard degrees of freedom at the early stages of high-energy collision in a simple setting, where the only nontrivial effects distinguishing the nuclear collision from an incoherent superposition of nucleon-nucleon ones are jet quenching, i.e. energy losses experienced by partons traversing the surrounding debris created in nuclear collision, and account-

ing for nuclear effects in the parton structure functions. Effects of rescattering and possible evolution of the initially produced parton system towards equilibrium are not included in this consideration.

To quantify the event-by-event asymmetry of transverse energy flow we study, as proposed in Ref. [37], the difference between the transverse energy deposited in some rapidity window $y_{min} < y_i < y_{max}$, and in two oppositely azimuthally oriented sectors having an angular opening $\delta\varphi$ each. The idea to use this quantity as a measure of the presence of semihard dynamics comes from the expectation that perturbative transverse energy production mechanisms have a built-in tendency of creating an event-by-event azimuthal asymmetry *in a fixed rapidity window*. For example, the partonic transverse energy flow occurring through binary parton collisions becomes, with increasing collision energy, more and more azimuthally unbalanced, because one of the two scattered partons just misses the rapidity window in question [37]. In the limit of high energies even the binary parton scattering at central rapidities as such becomes azimuthally unbalanced because of the growing contribution of primordial transverse momentum to particle production [38]. In contrast, one expects the soft transverse energy production mechanisms, e.g. string decays, to be more azimuthally balanced *locally in rapidity* on an event-by-event basis because of the small momentum transfer involved.

By benoting the transverse energy going into the 'upper' and 'lower' cones in a given event by $E_\perp^\uparrow(\delta\varphi)$ and $E_\perp^\downarrow(\delta\varphi)$, respectively, the asymmetry in transverse energy production in a given event is thus described by $\delta E_\perp(\delta\varphi)$:

$$\delta E_\perp(\delta\varphi) = E_\perp^\uparrow(\delta\varphi) - E_\perp^\downarrow(\delta\varphi). \tag{6.3}$$

An ensemble of collisions is characterized by an event-by-event probability distribution

$$P(\delta E_\perp|\delta\varphi) = \frac{d\,w(\delta E_\perp(\delta\varphi))}{d\,\delta E_\perp(\delta\varphi)}. \tag{6.4}$$

This distribution was calculated in Ref. [34] in the HIJING model for central Au+Au collisions at RHIC energy $\sqrt{s} = 200\,\mathrm{GeV}$ and central Pb+Pb collisions at LHC energy $\sqrt{s} = 5.5\,\mathrm{TeV}$ for $\delta\varphi = \pi$ and central rapidity interval $-0.5 < y < 0.5$. The distributions $P(\delta E_\perp|\pi)$ were calculated *both* at partonic level and at the level of final hadrons with semihard interactions and quenching on and off. This allowed one to separate the contribution of minijets as described by HIJING from the backgroun of soft processes. The resulting distributions for the LHC are shown in Fig. 6.9 with quenching turned on and the chosen value of the minijet's infrared cutoff $p_0 = 2\,\mathrm{GeV}$.

**Table 1**

| AA | $\sqrt{s}$ (GeV) | $p_0$ (GeV) | Asymmetry | $\sqrt{\langle \delta E^2 \rangle}$ (GeV) |
|---|---|---|---|---|
| Au+Au | 200 | 2 | hadrons (quenching on) | 16 |
| | | | hadrons (quenching off) | 17 |
| | | | partons | 18 |
| | | | soft hadrons | 7 |
| PbPb | 5500 | 2 | hadrons (quenching on) | 61 |
| | | | hadrons (quenching off) | 71 |
| | | | partons | 65 |
| | | | soft hadrons | 15 |
| PbPb | 5500 | 4 | hadrons (quenching on) | 69 |
| | | | partons | 76 |
| | | | soft hadrons | 16 |

The numerical values of the standard deviation $\sqrt{\langle \delta E_\perp^2 \rangle}$ characterizing the widths of the corresponding probability distributions are shown in Table 1, where for completeness we also show these standard deviations for the cases of quenching turned off and with a larger value for the infrared cutoff $p_0 = 4\,\mathrm{GeV}$

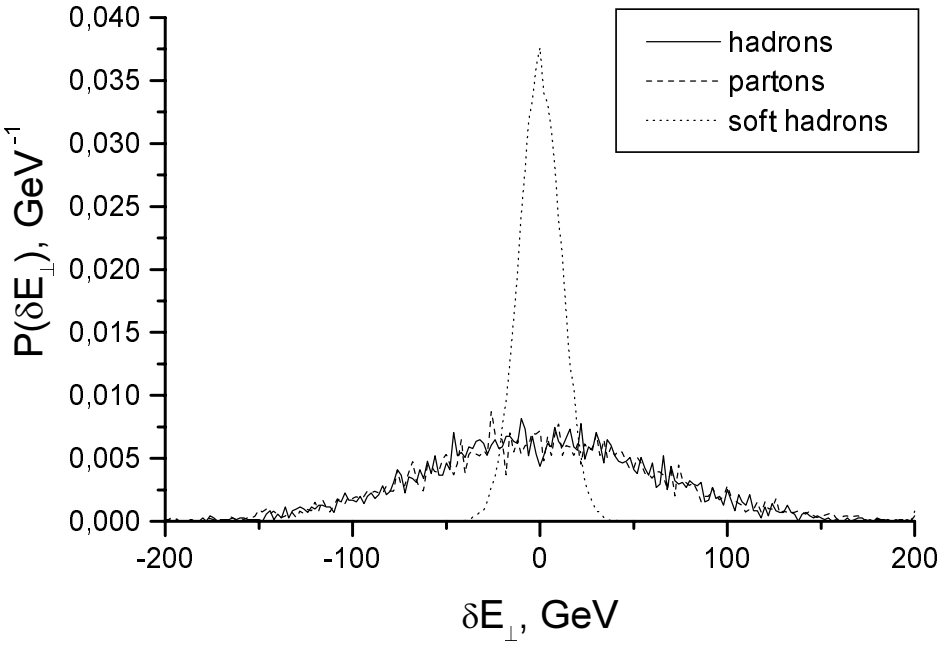


**Figure 6.9:** Probability distribution for azimuthal transverse energy imbalance in the unit rapidity window for PbPb collisions at LHC energy $\sqrt{s} = 5.5\,\text{TeV}$, $p_0 = 2\,\text{GeV}$, quenching on.

We see that the magnitude of the azimuthal asymmetry is essentially determined by the relative yield of the semihard (minijet) contribution. Switching off minijets, and thus restricting oneself to purely soft mechanisms, leads to a substantial narrowing of the asymmetry distribution; by the factor of 2.3 at RHIC and by the factor 4.1 at LHC energy, respectively, (these values correspond to the case of quenching turned on). Quite remarkably, the parton and final (hadronic) distributions of $\delta E_\perp$ in both cases practically coincide indicating that the contribution to transverse energy due to hadronization of the primordial parton system is, to a high accuracy, additive and symmetric in azimuthal angle and thus cancels out. We see that the transverse energy flow imbalance Eq. (6.3) is a sensitive indicator of the presence of primordial semihard parton dynamics that can be studied in calorimetric measurements in central detectors at the LHC.

As mentioned earlier, rescattering of produced partons, which is essential for possible evolution of the primordial partons towards equilibration, was not taken into account in the above consideration. In fact one expects parton rescattering to destroy at least some of the initial asymmetry of the transverse energy flow, making its measurement even more interesting.

#### 6.8.3.2 Fluctuations of conserved quantities

In this subsection we discuss the fluctuation of conserved quantities such as charge or baryon number. The advantage [20,21] of studying the fluctuation of conserved quantities is that their relaxation time in a thermal system is much slower than that of non-conserved quantities, since there is no process which can generate conserved quantum numbers from the vacuum or via particle collisions. A detailed discussion of the relaxation time of fluctuation of conserved quantities is provided in Ref. [26]. As a consequence, the fluctuation of conserved charges such as net electric charge or baryon number may provide information from deep inside the system created in these collisions, where possibly a system with different degrees of freedom existed.

In addition, the fluctuations of baryon number and charge are sensitive to the fractional charge/baryon number carried by the quarks in the QGP, and amy provide therefore an imporatnt signature for the

existence of a deconfined phase as will be discussed in detail below.

Of course, global charge conservation leads to vanishing fluctuations once the entire system is considered. But if only a small fraction of the produced particles are taken into account, the effect of global charge conservation plays a minor role and appropriate corrections can be applied.

To be specific, let us consider the fluctuation of the electric charge. The arguments for the baryon number are analogous and can be found in Ref. [20]. For simplicity let us assume that the QGP is made of non-interaction massless quarks and gluons. The fluctuations of the charge are given by

$$\left\langle (\delta Q)^2 \right\rangle = \left\langle Q^2 \right\rangle - \left\langle Q \right\rangle^2, \tag{6.5}$$

where $Q$ is the net charge measured in the acceptance. For a system of several particle species $i$ with charges $q_i$ and multiplicities $n_i$ we have

$$\begin{aligned} Q &= \sum_i q_i n_i, \\ \langle Q \rangle &= \sum_i q_i \langle n_i \rangle \end{aligned} \tag{6.6}$$

and

$$\left\langle (\delta Q)^2 \right\rangle = \sum_i (q_i)^2 \langle n_i \rangle + \sum_{i,k} c_{ik}^{(2)} \langle n_i \rangle \langle n_k \rangle q_i q_k, \tag{6.7}$$

where $c_{i,k}^{(2)}$ are the normalized two-particle correlation functions

$$c_{ii}^{(2)} = \frac{\langle n_i (n_i - 1) \rangle}{\langle n_i \rangle^2} - 1, \tag{6.8}$$

$$c_{ik}^{(2)} = \frac{\langle n_i n_k \rangle}{\langle n_i \rangle \langle n_k \rangle} - 1 \quad \text{if i} \neq \text{k}. \tag{6.9}$$

Obviously correlations introduced by particle interactions, such as resonances, affect the fluctuations [39–41]. And, therefore, as we shall discuss below the fluctuations my be used as means to measure particle correlations in these systems. If, on the other hand, the particles are uncorrelated, the second term of Eq.. 6.7 vanishes.

In a thermal system the charge fluctuations are given by the charge susceptibility:

$$VT\chi_Q = -T \frac{\partial^2 F}{\partial \mu_Q^2}, \tag{6.10}$$

which for a macroscopic system measures the response to external electric fields.

In the case of a free uncorrelated pion gas the charge fluctuations are then

$$\left\langle (\delta Q)^2 \right\rangle_{\pi-\text{gas}} = \langle N_+ \rangle + \langle N_- \rangle = \langle N_{ch} \rangle, \tag{6.11}$$

where $N_{ch}$ is the total number of charged particles. For a QGP, on the other hand, assuming uncorrelated quarks and gluons, one obtains

$$\left\langle (\delta Q)^2 \right\rangle_{\text{QGP}} = q_u^2 \langle N_u + N_{\bar{u}} \rangle + q_d^2 \langle N_d + N_{\bar{d}} \rangle = \frac{5}{18} \left\langle N_q \right\rangle, \tag{6.12}$$

where $N_q$ is the total number of quarks in the system. The contribution of heavy quarks can be neglected since their yield is suppressed.

Note that in the case of the QGP the charge fluctuations depend on the square of the fractional charge of the quarks. In order to expose the dependence on the fractional charge, one should divide the charge

fluctuations by the number of particles or the entropy carried by the system. A good measure for the entropy is the number of charged particles in the final state and thus the observable

$$\frac{\left\langle (\delta Q)^2 \right\rangle}{\langle N_{ch} \rangle} \tag{6.13}$$

should be sensitive to the fractional charges of the QGP. And indeed, using $N_{ch} \simeq N_q + N_g$ (which follows from the assumption of entropy conservation), where $N_g$ is the number of gluons (for detailed discussion see Ref. [21]) one obtains

$$\frac{\left\langle (\delta Q)^2 \right\rangle}{\langle N_{ch} \rangle}_{\text{QGP}} \simeq 0.2 \tag{6.14}$$

and

$$\frac{\left\langle (\delta Q)^2 \right\rangle}{\langle N_{ch} \rangle}_{\pi-\text{gas}} = 1 \tag{6.15}$$

for the pion gas.

Correcting for quantum statistics and taking hadronic resonances into account, which introduce correlation terms (see Eq. 6.7), one has for the hadron gas

$$\frac{\left\langle (\delta Q)^2 \right\rangle}{\langle N_{ch} \rangle}_{\text{hadron}-\text{gas}} \simeq 0.75. \tag{6.16}$$

On the quark-gluon plasma side, one can actually consult Lattice QCD calculations, which are available for the charge fluctuations as well as for the entropy. In this case one finds [21]

$$\frac{\left\langle (\delta Q)^2 \right\rangle}{\langle N_{ch} \rangle}_{\text{QGP}} \simeq 0.25 - 0.4, \tag{6.17}$$

where the uncertainty is due to the way in which entropy is related to the number of charged particles (see Refs. [20, 21]).

To access this observable in the experiment it is *not* sufficient to simply measure the charge fluctuations and the number of charged particles separately. As can be seen from Eq. 6.7 the magnitude of the charge fluctuations scales with the number of charged particles in the system, i.e. it scales with the system size. Therefore fluctuations of the system size, or impact parameter fluctuations, which are present even if centrality cuts are applied, will contribute to the charge fluctuations. Of physical interest, however, are the charge fluctuations due to density fluctuations. Thus, the effect of volume fluctuations has to be removed by an appropriate choice of observables.

Within this context two measures of fluctuations are discussed: the $\Phi_q$ measure [24] and the $\tilde{D}$ measure [42]. It was shown [24] that the $\Phi_q$ measure is less sensitive to the biasing effects than the originally proposed $\tilde{D}$ measure. Both are sensitive to the hypothetical suppression of charged fluctuations due to QGP creation.

Finally, let us mention that similar information may also be obtained by measuring so-called balance functions [41, 43].

#### 6.8.3.3 Long-range forward-backward $p_t$ and multiplicity correlations

Soft and semi-hard parts of the multi-particle production at high energy are successfully described in terms of colour strings stretched between the projectile and target [44, 45]. The hadronization of these strings produces the observed hadrons. In the case of nuclear collision, with growing energy and atomic

number of colliding particles, the number of strings grows and one has to take into account the interaction between strings in the form of their fusion and/or percolation. [46]- [52].
Around the percolation threshold [49], strong fluctuations in the number of strings with a given colour should appear. This will produce large fluctuations in a number of different observables in an event-by-event analysis. Scanning in the impact parameter space for the PbPb collisions provides the possibility to change the density of the overlapping strings by moving from the most peripheral to the central collisions (see Ref. [29] for details). Therefore the onset of the critical fluctuations relevant to the string fusion and/or percolation could be obtained in the very first days of ALICE running from the observation of correlation coefficient vs. event centrality.
The impact parameters determination in ALICE by the Zero Degree Calorimeter can determine the centrality of collisions with an accuracy better then 1 fm in the region of impact parameters below 11 fm for Pb+Pb collisions. We expect [53] to use the FMD rapidity distribution information for the purpose of impact parameter determination at the larger values as was suggested earlier [54, 55].
We propose [29, 56] to measure the following types of long-range forward-backward correlations (FBC) in ALICE at the LHC: long-range FBC of mean multiplicity vs. multiplicity (*n*-*n* FBC), mean $p_t$ vs. $p_t$ ($p_t$-$p_t$ FBC), and mean $p_t$ vs. multiplicity ($p_t$-*n* FBC).
For a long time the long-range *n*-*n* FBCs in p+p and p+$\overline{\text{p}}$ collisions have been studied experimentally and theoretically (see Ref. [29] for references). Usually the average charged particle multiplicity in the backward hemisphere as a function of the *event* multiplicity in the forward hemisphere is studied.

The data obtained at ISR, SPS and Fermilab energies can be almost perfectly represented by a linear function

$$\langle n_B \rangle_{n_F} = a + b_{cor} n_F, \tag{6.18}$$

the strength of the correlation measured by the coefficient $b_{cor}$.
Similarly to *n*-*n* FBC (6.18) one can study $p_t$-$p_t$ FBC

$$\langle p_{tB} \rangle_{p_{tF}} = \alpha + \beta_{cor}, \tag{6.19}$$

here the $p_{tF}$ is the average $p_t$ of charged particles produced in the forward pseudorapidity window $\Delta y_F$ in a given event and the $p_{tB}$ is the same for the backward window $\Delta y_B$. The $\langle ... \rangle_{p_{tF}}$ means averaging over events with fixed $p_{tF}$ and $\langle ... \rangle$ means averaging over all events (see Ref. [29] for details).

Another possibility that we propose to be used in ALICE [29] includes the mean $p_t$-multiplicity FBC. This is a nice combination of the event-by-event $p_t$ measurements by the ITS and TPC, and of the multiplicity information coming from the FMD. For mixed $p_t$-*n* FBC one can write

$$\langle p_{tB} \rangle_{nF} = \bar{a} + \bar{b}_{cor} n_F, \tag{6.20}$$

where $\bar{b}_{cor}$ is $p_t$-*n* correlation coefficient.

*Mean $p_t$ - multiplicity FBC in PSM-1*

The Parton String Model event generator (PSM-1) [54, 57] allows Monte Carlo simulations with and without string fusion, and therefore one can choose the most adequate correlation variables for the registration of the possible string fusion in ALICE. We perform the simulations in all three cases - for *n*-*n*, $p_t$-$p_t$ and $p_t$-*n* FBC. The clearest appearance of the string fusion phenomenon was found in the case of $p_t$-*n* FBC [29].

First of all the results obtained using the PSM-1 generator, as was expected [58], indicate noticeably increased $p_t$ values (up to 0.5 GeV/c) in the central pseudorapidity region.
Secondly a strong rise of the $p_t$-*n* correlation coefficient in the case of string fusion in the region where the percolation is expected (region of the impact parameter 10-15 fm for the Pb+Pb collisions at LHC energies, see Fig. 6.10) is observed. This is also illustrated by the correlation function for the 10-15 fm impact parameter region (see Fig. 6.11) calculated with and without string fusion.

*Long-range FBC studies at ALICE*

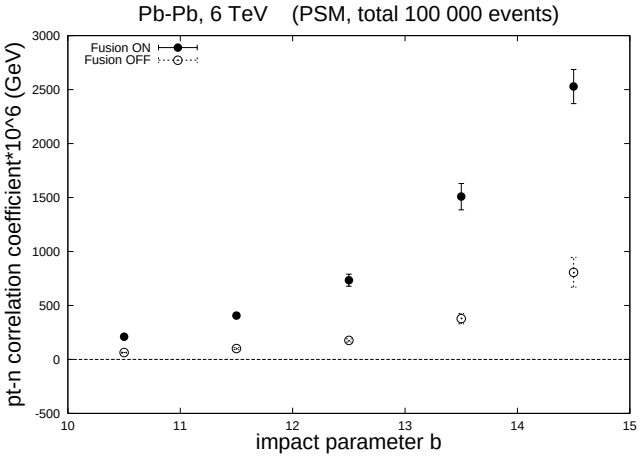


**Figure 6.10:** The $p_t$-multiplicity FBC in the peripheral region in Pb+Pb collisions at 6 TeV/nucleon. The $p_t$-multiplicity correlation coefficient $\overline{b}_{cor}$ (see Eq. 6.20) for pseudorapidity windows $\Delta y_B = (-0.8, 0)$ and $\Delta y_F = (2, 4)$ as a function of the impact parameter $b \in (10, 15)$ calculated in 1 fm steps. (MC simulations, PSM, 100 000 events).

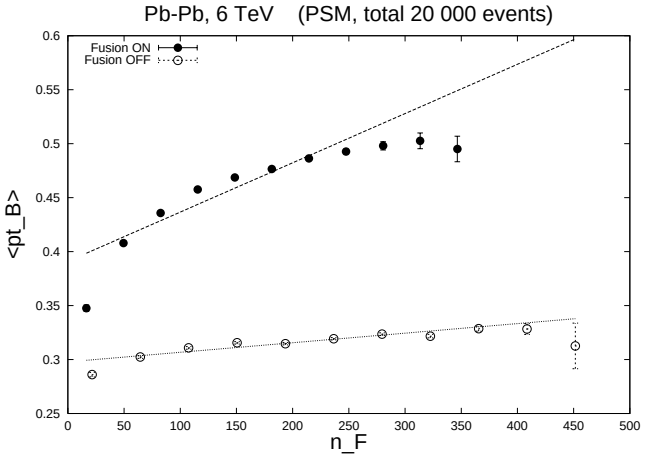


**Figure 6.11:** The $p_t$-multiplicity FBC in peripheral (impact parameter $b \in (10, 15)$) Pb+Pb collisions at 6 TeV/nucleon. The $\langle p_{tB} \rangle_{n_F}$ - average $p_t$ of charged particles (over all events with fixed $n_F$) produced in the backward pseudorapidity window $\Delta y_B = (-0.8, 0)$ as a function of the *event* multiplicity $n_F$ in the forward $\Delta_F = (2, 4)$ pseudorapidity windows. (MC simulations, PSM, 20 000 events).

Event-by-event measurements of the $p_t$ distributions in ALICE could be done only in the central pseudorapidity acceptance (-0.9, 0.9) using the information obtained from the ITS and the TPC. Therefore we can combine the central rapidity data with the detailed event-by-event information on multiplicity of charged particles obtained by the FMD in a wide pseudorapidity range. FMD can provide also the azimuth ($\phi$) distributions that could be useful for possible hard-jet discrimination.

Therefore we can study $p_t$ multiplicity FBC at LHC energies choosing the first pseudorapidity window in the central acceptance region (-0.9, 0.9) for the $p_t$ data, and the second window within the pseudorapidity intervals (-5.1,-1.7) and/or (1.7, 3.4) for multiplicities measured with the Si-FMD.
The TPC and FMD data off-line analysis makes it possible to discriminate the hard processes like jets in ALICE (in the present Monte Carlo simulation study these jets in the PSM generator were simply switched off):
a) by cuts in $p_t$ used in correlation studies (e.g. cuts of the high values at the level of 1-1.5 GeV/c could be applied for the ITS and the TPC data);
b) by an exclusion of the windows in $\phi$ distributions with indications of hard jets formation (the FMD multiplicity data).

#### 6.8.3.4 Temperature fluctuations

The concept of temperature plays a key role in the description of relativistic heavy-ion collisions because the matter produced at early stages of the collision achieves, at least to some extent, local thermodynamic equilibrium. The question arises whether there is a unique temperature of the system at freeze-out or whether the temperature fluctuates from one collision to another [31]. We argue here that the high-precision measurements of the event-by-event temperature fluctuations are feasible in the ALICE experiment. We do not discuss the thermodynamic interpretation of the $T$ fluctuations which appears to be a rather controversial matter [59].

The temperature can be inferred from the experimental data in several ways. In particular, one analyses the $p_T-$distribution which is usually taken in the form

$$\frac{dN}{d^2p_T} \propto \exp\left(-\frac{m_T}{T}\right) , \tag{6.21}$$

where $m_T \equiv \sqrt{m^2+p_T^2}$ with $m$ being the particle mass; $T$ is the *effective* temperature which, as commonly accepted, see for example Ref. [60], combines the genuine temperature $T$ and transverse flow velocity $u$ according to the approximate relation $T = T\sqrt{(1+u)/(1-u)}$ [61]. Further, we consider the fluctuations of $T$ rather than $T$. Obviously, the fluctuations of $T$ and $u$ both contribute to that of $T$. Since the discussion of thermodynamic meaning of the temperature fluctuations is beyond the scope of this note, the distinction between $T$ and $T$ is not important for us.

We discuss below how to detect the temperature fluctuations and start with a simple observation that the fluctuations influence the shape of the $p_T$ distribution. It has been shown [62] that the $T$ fluctuations in the exponential formula (6.21) lead in a natural way to the power-like form which is known as the Lévy distribution. Indeed, averaging the exponential formula over the fluctuations of $1/T$ which follow the gamma distribution, one gets

$$\left[1-(1-q)\frac{m_T}{T_0}\right]^{\frac{1}{1-q}} , \tag{6.22}$$

where $1/T_0 \equiv \langle 1/T\rangle$. The parameter $q$ - the so-called entropic index or nonextensivity parameter in Tsallis statistics [63] - is connected to the size of the fluctuations. Namely,

$$q-1 = \frac{\langle 1/T^2\rangle - \langle 1/T\rangle^2}{\langle 1/T\rangle^2} \cong \frac{\langle T^2\rangle - \langle T\rangle^2}{\langle T\rangle^2} ,$$

where the second approximate equality holds for sufficiently small fluctuations. When $q = 1$ there are no temperature fluctuations and the exponential formula is restored.

The distribution of the Lévy type (6.22) has been observed in inclusive processes [64], which, however, do not provide an unambiguous answer as to what is the source of such a behaviour. This can be done by performing an event-by-event analysis of the data. The point is that when $T$ fluctuates from event to event, the $p_T$ distribution in a single event should differ from the $p_T$ distribution averaged over many events. In particular, if the single-event $p_T$ distribution is given by the exponential formula (6.21) the averaged one is that of Lévy (6.22). As shown in Ref. [65], a very large multiplicity of the central Pb+Pb collisions allows one to observe the difference for $q-1$ as small as 0.05.

Let us now discuss a method that was proposed in Ref. [66] and developed in Ref. [67], to study $T$ fluctuations more quantitatively. The temperature variance can be found by measuring the event's transverse mass defined as

$$\mu_T = \frac{1}{N}\sum_{i=1}^{N} m_T^i \,,$$

where $N$ denotes the event's multiplicity and $m_T^i$ is the transverse mass of $i$-th particle. If the single particle $p_T$ distribution is of the form (6.21) the event's temperature is expressed through $\mu_T$ as

$$T = \frac{1}{4}\left[\sqrt{4m\mu_T - 4m^2 + \mu_T^2} + \mu_T - 2m\right] .$$

Thus, measuring $\mu_T$ on the event-by-event basis one can get $V(T) \equiv \langle T^2\rangle - \langle T\rangle^2$. However, the statistical fluctuations due to the finite event multiplicity have to be subtracted from the result. The point is that even when the genuine temperature does not fluctuate at all, the observed one does vary because the number of registered particles is not infinite.

When the genuine temperature is fixed and the particles are independent from each other, the variance of $T$ is fully determined by statistical fluctuations. In the events of multiplicity $N$, it equals

$$V_s(T) = \frac{1}{16}\left[\frac{2m + \langle\mu_T\rangle}{\sqrt{4m\langle\mu_T\rangle - 4m^2 + \langle\mu_T\rangle^2}} + 1\right]^2 \frac{V_1(m_T)}{N} \,,$$

where $V_1(m_T)$ is the variance of the single particle $m_T$ distribution and

$$V_1(m_T) = \frac{6T^3 + 6T^2 m + 3Tm^2 + m^3}{T+m} - \left(\frac{2T^2 + 2Tm + m^2}{T+m}\right)^2 .$$

The variance $V_s(T)$ should be subtracted from the observed $T$ variance $V(T)$ to eliminate the statistical fluctuations. We have performed [67] a simple simulation to see how well the subtraction procedure works. It appears that for $N$ as small as 10 the value of $q > 1.05$ can be unambiguously observed provided the single-particle $p_T$ distribution is indeed described by Eq. (6.21).

The temperature fluctuations can also be observed by analysing the event-by-event $p_T$ fluctuations by means of the $\Phi$ measure [68]. $\Phi(p_T)$ for fluctuating $T$ was computed in [67]. Here, we sketch the derivation of the result. Let $P_{(T)}(p_T)$ denote the single-particle transverse momentum distribution in events with temperature $T$ which is assumed to be independent of the event's multiplicity $N$. Then, the inclusive transverse momentum distribution reads

$$P_{\rm incl}(p_T) = \int_0^\infty dT\; P(T)\, P_{(T)}(p_T) \,,$$

where $P(T)$ describes the temperature fluctuations. The $N$ particle transverse momentum distribution in the events of multiplicity $N$ is assumed to be the $N$ product of $P_{(T)}(p_T)$ weighted by the multiplicity and temperature distributions. Then, one finds

$$\langle Z^2\rangle = \sum_N P_N \int_0^\infty dT\; P(T) \int_0^\infty dp_T^1\, P_{(T)}(p_T^1) \ldots \int_0^\infty dp_T^N\, P_{(T)}(p_T^N) \times \left(p_T^1 + \ldots + p_T^N - N\overline{p_T}\right)^2 ,$$

where $P_N$ is the multiplicity distribution. In the limit $m = 0$, the $p_T$ distribution (6.21) acquires a simple exponential form and one easily computes $\overline{z^2}$ and $\langle Z^2 \rangle$. Assuming additionally that the $N$ and $T$ fluctuations are small, one gets a very simple result:

$$\Phi(p_T) = \sqrt{2}\,\langle N \rangle\,\frac{\langle T^2 \rangle - \langle T \rangle^2}{\langle T \rangle} = \sqrt{2}\,\langle N \rangle\,\langle T \rangle\,(q-1)\,. \tag{6.23}$$

Thus, $\Phi$ linearly depends on the temperature variance.

We have presented here three methods of studing the temperature fluctuations. We believe that by combining all of them one can get an unambiguous answer whether event-by-event temperature fluctuations are present in relativistic heavy-ion collisions, and if so, how large the fluctuations are.

#### 6.8.3.5 Disoriented chiral condensate

*i. What is DCC and how to detect it*

Observation in cosmic-ray experiments of events with extreme isospin imbalance among secondary particles ('centauros' with dominating hadronic component and 'anti-centauros' with dominating electromagnetic component) [33, 69] calls for an explanation. An interesting hypothesis is the creation of a 'disoriented chiral condensate' (DCC) - a meta-stable state resulting from the cooling down of the quark-gluon plasma [32]. Such a state appears in both linear and non-linear $\sigma$-models which are simplified versions of the full chiral effective theory. It may have a large isospin vector oriented in any direction in isospace, and thus it may be a source of secondary pions with any isospin configuration.

A DCC state may occupy the full available phase space or only a part of it, and thus it may constitute a source of all secondary pions or only of small fraction of them. Some theoretical models [70] predict 'DCC domains' of sizes 3-4 fm in radius, emitting 50-200 pions. Such a source may be situated in the central or in any other kinematic region, and the pion emission pattern might be statistical or coherent ('pion laser' [71]). If the pion emission from DCC is indeed coherent, the pions will be collimated in a limited region of phase space and will have small relative transverse momenta. In this case one would expect to find 'jet-like' structures with high isospin imbalance. One should, however, keep in mind that such finding, compatible with the expected characteristics of DCC, would not explain the 'centauro' events which are characterized, on the contrary, by high transverse momenta, of the order of 1-2 GeV/c [33].

In view of these unclear predictions it seems plausible to search for DCC in various phase space regions, not only in the most forward one in which 'centauros' have been observed in cosmic rays, and to look at various event characteristics.

A large isospin imbalance among the produced pions is considered as the primary signature of DCC. The ratio of neutral to charged pions created in any statistical emission process can be described by a binomial distribution that becomes rather narrow for high multiplicities, with a mean value of about $1/2$. For the fraction of neutral pions among all pions, $f = N_{\pi^o}/N_\pi$ , a similar narrow distribution with the mean value of about $1/3$ is expected. For DCC the distribution of this ratio is $P(f) = 1/2\sqrt{f}$ which is very wide and consequently large event to event fluctuations of $f$ are expected. Thus the prescription for finding DCC is to measure photons and charged hadrons within a common acceptance.

Several methods of analysis leading to this goal have been proposed:
a) $N_\gamma - N_{ch}$ correlation,
b) discrete wavelet analysis,
c) power spectrum analysis,
d) 'robust' observables,
e) event-shape analysis.
Below we give a short description of these methods.

**a)** $N_\gamma - N_{ch}$ **correlation**

This is the most straightforward method. In 'normal' events $N_\gamma$ and $N_{ch}$ are correlated. In events with DCC this correlation will be distorted: anomalous enhancement of $N_\gamma$ or $N_{ch}$ will appear. The effect can be quantified in terms of the scaled variable $S_z = D_z/\sigma(D_z)$ where $D_z$ is the distance of a point in the $N_\gamma - N_{ch}$ plane to the correlation axis, and $\sigma(D_z)$ is the dispersion of the $D_z$ distribution for 'normal' events. The correlation can be studied in full detector acceptance, or in smaller regions.

**b) Discrete wavelet analysis**

In the Discrete Wavelet Analysis (DWA), also called Discrete Wavelet Transformation (DWT), one studies fluctuations in the neutral pion fraction, $f = N_{\pi^o}/N_\pi$, in small bins, at different scales (different binning). The distribution of the obtained wavelet coefficients for 'normal' events should be Gaussian, while the occurrence of a DCC makes the distribution much wider and non-Gaussian. This increase in width is a sensitive parameter. The method allows one to pick up fluctuations in small bins.

**c) Power spectrum analysis**

In this approach one computes the fraction $f = N_\gamma/N_{ch}$ for a certain window, e.g. a window in azimuthal angle $\phi$, and this window is then displaced by a small amount, $f$ is recalculated, etc. The power spectrum is the square of the Fourier transform of the $(f(\phi) - f_o(\phi))$ distribution where $f_o(\phi)$ is the distribution for 'normal' events. It shows a complicated pattern, with narrow peaks indicating local fluctuations in the original distribution.

**d) 'Robust' variables**

The analysis uses the ratios of factorial moments

$$R_{i,1} = \frac{F_{i,1}}{F_{i+1,0}}$$

where

$$F_i = \frac{< N(N-1)...(N-i+1) >}{< N >^i}$$

and

$$F_{i,j} = \frac{< N_{ch}(N_{ch}-1)...(N_{ch}-i+1)N_\gamma(N_\gamma-1)...(N_\gamma-j+1) >}{< N_{ch} >^i < N_\gamma >^j}$$

The variables $R$ have been named 'robust variables' because the detection efficiencies, often difficult to estimate (especially for photons), cancel out and thus do not influence the results. For 'normal' events (statistical uncorrelated emission) $R_{i,1} = 1$, while for DCC $R_{i,1} = 1/(i+1)$ - a remarkable difference for all $i \geq 1$. The analysis can be done inclusively or event-by-event (for high multiplicity events, as expected in ALICE).

**e) Event-shape analysis**

This method combines the wavelet technique and flow analysis. The flow direction is found separately for charged particles and photons and compared. For a DCC component a difference between the two directions might be expected.

*ii. Experimental search for DCC*

The first attempt to look for DCC in relativistic nuclear collisions was made by the CERN NA49 Collaboration [72]. For semi-central Pb+Pb collisions at 158 A GeV the ratio of electro-magnetic to hadronic transverse energy, $E_T^{EM}/E_T^{HAD}$, was calculated for each event using the radially and azimuthally segmented cylindrical calorimeter. The distribution of this ratio was found compatible with that predicted by the VENUS model, with the mean value close to 0.3, and tails not showing the presence of any 'anomalous' events.

A dedicated experiment, MiniMax, was set up at the Tevatron at Fermilab to study p+$\bar{p}$ collisions at $\sqrt{s}$ = 1.8 TeV [73]. Their detector was composed of 24 MWPCs with a removable lead gamma converter, and a segmented electro-magnetic calorimeter behind it. The detector had a very small angular acceptance: a cone with axis at $\eta$ = 4.1, with half-angle 0.65. The authors developed and used the method of 'robust' variables for data analysis. No evidence for DCC was found at a few per cent level.

A thorough DCC search in Pb+Pb collisions at 158 A GeV was performed by the WA98 Collaboration at CERN [74]. The Silicon Pad Multiplicity Detector and the Photon Multiplicity Detector were used to measure the charged and neutral multiplicities for each event, and the Midrapidity Calorimeter for the determination of event centrality. The data were analysed in terms of the dispersion of points with respect to the $N_\gamma - N_{ch}$ correlation axis (the $S_z$ variable). No DCC signal was observed and the upper limit for DCC production at 90% CL was established as a function of the fraction of DCC pions among all pions produced.

The wavelet (DWT) analysis of Pb+Pb events at 158 A GeV performed by the NA44 Collaboration [75] revealed no local charge density fluctuations. This group, however, uses only information on secondary charged hadrons (data from multi-pad Si array) and their results might be relevant to DCC search only if DCC is produced locally in small 'droplets'.

The results of a DCC search in Au+Au collisions at c.m. energy up to $\sqrt{s_{NN}}$= 200 GeV can be expected soon from experiments at RHIC, especially from the complex hybrid detectors STAR and PHENIX.

*iii. Detection of DCC in ALICE*

The ALICE detector makes it possible to search for DCC by comparing the emission of charged and neutral pions in two distinct regions of phase space:
a) central region (PHOS + TPC): $-0.12 < \eta < 0.12$ , $\Delta\phi = 100^o$
b) intermediate region (PMD + FMD): $1.8 < \eta < 2.6$ , full azimuth

**a) Central region - PHOS+TPC**

In this region determined by the acceptance of the photon spectrometer PHOS, photons will be recorded by the PHOS [76], and charged pions by the TPC [77]. The PHOS detector has an area of about 8 m$^2$ and is composed of 17 280 lead tungstate crystals of 2.2x2.2 cm$^2$ face area, which makes for a good space resolution. The photon detection efficiency is close to 100%. Charged pions will be recorded in the TPC, together with the momentum measurement. If one takes the highest estimate for the number of charged particles produced per unit of rapidity, at midrapidity, to be about 8000, then about 550 charged pions and 550 photons might be expected within the PHOS acceptance.

**b) Intermediate region - PMD+FMD**

PMD [78] is the preshower photon detector with active area of about 10 m$^2$ , subdivided into 200 000 cells, each cell having an area of 1 cm$^2$. It will detect photons with an efficiency of about 70%. In conjunction with the forward multiplicity detector FMD measuring the multiplicity of charged particles, in a common part of phase space, it is well suited for a search for DCC formation. The expected number of photons and charged pions in the PMD acceptance is about 4000. Due to this large multiplicity, a search for DCC in more restricted regions of phase space can also be performed.

*iv. Conclusions*

The ALICE detector offers possibilities to search for DCC in various pseudorapidity regions, central and intermediate, in cells of various sizes. The estimate of the level of sensitivity to a possible DCC signal would require appropriate simulation studies.

#### 6.8.3.6 Colour collective phenomena

A copious production of partons, mainly gluons, due to hard and semi-hard processes, is expected in heavy-ion collisions at the LHC. One deals with the many-parton system at the early stage of the collision. The system is on the average locally colourless but random fluctuations can break the neutrality. Since the system is initially far from equilibrium, specific colour fluctuations can exponentially grow in time and then noticeably influence the system evolution. The very existence of such fluctuations would be a clear manifestation of the quark-gluon plasma where the colour forces act well beyond the confinement scale.

As argued in a series of papers [30], the colour plasma instabilities can indeed occur due to the strongly elongated parton momentum distribution. These instabilities, in particular the so-called filamentation instability, generate collective transverse flow in heavy-ion collisions. The occurrence of the filamentation breaks the azimuthal symmetry of the system. The azimuthal orientation of the wave vector will change from one collision to another, while the instability growth will lead to the energy transport along this vector. Consequently, one expects significant variation of the transverse energy as a function of the azimuthal angle. This expectation is qualitatively different from that based on the parton cascade simulations [79], where the fluctuations are strongly damped due to the large number of uncorrelated partons. On account of the collective character of the filamentation instability, the azimuthal symmetry will be presumably broken by a flow of a large number of particles with relatively small transverse momentum. The jets produced in hard parton-parton interactions also break the azimuthal symmetry. However, a few particles with large transverse momentum break the symmetry in this case [80]. One also expects the generation of the collective transverse motion as a result of the anisotropic pressure gradient [81, 82]. The flow is of the hydrodynamic nature and, in contrast to the colour instability driven transport, it is strongly correlated with the collision plane orientation. This gives a chance distinguishing the two phenomena.

The collective flow can be studied by means of various methods. We propose to use the fluctuation measure $\Phi$ [11] which has been proven to be very sensitive to the collective effects [16, 83].

# References

## Chapter 6.8


[1] J. C. Collins and M. J. Perry, Phys. Rev. Lett. **34**, 151 (1975),
E. V. Shuryak, Phys. Rep. **C61**, 71 (1980) and **C115**, 151 (1984).

[2] for recent review see H. Heiselberg, Physics Reports **351** (2001) 161.

[3] R. Stock, *Event–by–Event Analysis of Ultrarelativistic Heavy Ion Collisions*, in Proceedings of the NATO Advanced Study Workshop on Hot Hadronic Matter: Theory and Experiment, Divonne-les-Bains, France, 27 June–1 July 1994.

[4] S. Afanasiev et al. (NA49 Collab.), Nucl. Instrum. Meth. **A430**, 210 (1999).

[5] M. Gaździcki and M. I. Gorenstein, Acta Phys. Polon. **B30** (1999) 2705 and references therein.

[6] F. Becattini, Z. Phys. **C69**, 485 (1996),
F. Becattini and U. Heinz, Z. Phys. **C76**, 269 (1997),
F. Becattini, M. Gaździcki and J. Sollfrank, Eur. Phys. J. **C5**, 143 (1998).

[7] G. Odyniec, Nucl. Phys. **A638**, 135c (1998).

[8] H. Appelshauser et al. (NA49 Collab.), Phys. Lett. **B459**, 679 (1999).

[9] S. V. Afanasiev et al., Phys. Rev. Lett. **86**, 1965 (2001).

[10] St. Mrówczyński, Phys. Lett. **B439**, 6 (1998).

[11] M. Gaździcki and St. Mrówczyński, Z. Phys. **C54** (1992) 127.

[12] C. Pruneau, S. Gavin, S. Voloshin, Phys. Rev. **C66**, 044904 (2002).

[13] C. Alt et al. (NA49 Collab.), e-Print Archive: hep-ex/0311009.

[14] K. Adcox et al. (PHENIX Collab.), Phys. Rev. **C66**, 024901 (2002).

[15] E. G. Ferreiro, F. del Moral, C. Pajares, e-Print Archive: hep-ph/0303137.

[16] F. Liu et al., Eur. Phys. J. **C8**, 649 (1999).

[17] A. Capella, E.G. Ferreiro and A.B. Kaidalov, hep-ph/9903338 and
A. Capella, Acta Phys. Polon. **B30** (1999) 3541, hep-ph/9910219.

[18] Proceedings of the XV–th International Conference on Ultra–Relativistic Nucleus–Nucleus Collisions, Stony Brook, USA, January 2001.

[19] D. Adamova et al. (CERES Collab.), e-Print Archive: nucl-ex/0305002

[20] M. Asakawa, U. Heinz, B.Muller, Phys. Rev. Lett. **85** (2000) 2072.

[21] S. Jeon and V. Koch, Phys. Rev. Lett. **85** (2000) 2076.

[22] K. Adcox et al. (PHENIX Collab.), nucl-ex/0203014, to be published in Phys. Rev. Lett.

[23] S. Voloshin et al. (STAR Collab.), nucl-ex/0109006.

[24] J. Zaranek, Phys. Rev. C **66** (2002) 024905 [arXiv:hep-ph/0111228].

[25] S. Mrowczynski, Phys. Rev. C **66** (2002) 024904 [arXiv:nucl-th/0112007].

[26] E. Shuryak and M.A. Stephanov, Phys. Rev. **C63** (2001) 064903.

[27] M. M. Aggerwal et al. (WA98 Collab.), Phys. Lett. **B420** (1998) 169.

[28] S. Mrowczynski, Acta Phys. Polon. **B31** (2000) 2065, nucl-th/9907099.

[29] P.A.Bolokhov, M.A.Braun, G.A.Feofilov, V.P.Kondratiev, V.V.Vechernin,
Internal Note/PHY, ALICE-INT-2002-20 (2002) 16p.

[30] St. Mrówczyński, Phys. Lett. **B314** (1993) 118;
*ibid.* **B393** (1997) 26; Phys. Rev. **C49** (1994) 2191;
St. Mrówczyński and M. Thoma, Phys. Rev. **D62** (2000) 036011.

[31] L. Stodolsky, Phys. Rev. Lett. **75**, 1044 (1995);
E.V. Shuryak, Phys. Lett. B **423**, 9 (1998);
M. Stephanov, K. Rajagopal, and E.V. Shuryak, Phys. Rev. D **60**, 114028 (1999).

[32] J.D.Bjorken, K.L.Kowalski and C.C.Taylor, SLAC-PUB-6109, April 1993.
[33] For an extensive review on ”centauros” and related phenomena see E.Gładysz-Dziaduś, INP Report No.1879/PH, Cracow, 2001.
[34] A. Leonidov and D. Ostrovsky, *Phys. Rev.* **C63** (2001), 03791.
[35] A. Leonidov, “On Transverse Energy Production in Hadron Collisions”, **BNL-NT-00/12**.
[36] X.-N. Wang and M. Guylassy, *Phys. Rev.* **D44** (1991), 3501; **D45** (1992), 844;
*Comput. Phys. Commun.* **83** (1994), 307.
[37] A. Leonidov and D. Ostrovsky, *Eur. Phys. Journ.* **C16** (2000), 683
[38] A. Leonidov and D. Ostrovsky, *Phys. Rev.* **D62** (2000), 094009
[39] S. Jeon and V. Koch, Phys. Rev. Lett. **83** (1999) 5435.
[40] A. Bialas, Phys. Lett. B **532** (2002) 249 [arXiv:hep-ph/0203047].
[41] S. y. Jeon and S. Pratt, Phys. Rev. C **65** (2002) 044902 [arXiv:hep-ph/0110043].
[42] M. Bleicher, S. Jeon, and V. Koch, Phys. Rev. **C62** (2000) 061902.
[43] S. A. Bass, P. Danielewicz, S. Pratt, Phys. Rev. Lett. **85** (2000) 2689.
[44] A. Capella, U. P. Sukhatme, C.–I. Tan and J. Tran Thanh Van,
Phys. Lett. **B81** (1979) 68; Phys. Rep. **236** (1994) 225.
[45] A.B.Kaidalov, Phys. Lett., **116B** (1982) 459;
A.B.Kaidalov K.A.Ter-Martirosyan, Phys. Lett., **117B** (1982) 247.
[46] M.A.Braun and C.Pajares, Phys. Lett. **B287** (1992) 154;
Nucl. Phys. **B390** (1993) 542, 549;
N.S.Amelin, M.A.Braun and C.Pajares, Phys. Lett. **B306** (1993) 312;
Z.Phys. **C63** (1994) 507.
[47] N.S.Amelin, N.Armesto, M.A.Braun, E.G.Ferreiro and C.Pajares,
Phys. Rev. Lett. **73** (1994) 2813.
[48] N.Armesto, M.A.Braun, E.G.Ferreiro and C.Pajares,
Phys. Rev. Lett. **77** (1996) 3736.
[49] M.A.Braun, C.Pajares and J. Ranft.
Int. J. of Mod. Phys. **A14** (1999) 2689; hep-ph/9707363.
[50] M.Nardi and H.Satz, Phys. Lett. **B442** (1998) 14;
H.Satz, Nucl. Phys. **A661** (2000) 104c.
[51] M.A.Braun, C.Pajares and V.V.Vechernin. Phys. Lett. **B493** (2000) 54.
[52] M.A.Braun and C.Pajares, Eur. Phys. J. **C16** (2000) 349.
[53] G. Feofilov, *Experimental Studies of Long-Range Forward-Backward $p_t$ and Multiplicity Correlations at ALICE*; V. Vechernin *Forward-Backward Correlations in Relativistic Heavy Ion Collisions*. Reports at XVI International Baldin Seminar on High Energy Physics Problems, Dubna, Russia, June 10-15, 2002.
(See abstracts in ”Relativistic Nuclear Physics and Quantum Chromodynamics”, JINR, Dubna, 2002, pp.115,116.)
[54] ALICE Collaboration: *Technical Proposal for A Large Ion Collider Experiment at the CERN LHC*, preprint CERN/LHCC/95-71 (1995)
[55] G.A. Feofilov, V.P. Kondratiev, T.A. Tulina
Internal Note/FMD/SIM, ALICE-INT-2002-03 (2002) 14p.
[56] Braun M.A., Pajares C. and Vechernin V.V.
Internal Note/FMD, ALICE-INT-2001-16 (2001) 13p.
[57] N.S.Amelin, N.Armesto, C.Pajares and D.Sousa,
String Fusion Model: PSM-1.0 User’s Manual, (2000);
N. S. Amelin, N. Armesto, C. Pajares and D. Sousa, Eur.J.Phys. **C22** (2001) 149.
[58] M.A.Braun and C.Pajares, Phys. Rev. Lett. **85** (2000) 4864.
[59] C.Kittel, Phys. Today **5** (1988) 93;
B.B. Mandelbrot, Phys. Today **1** (1989) 71;

T.C.P. Chui, D.R. Swanson, M.J. Adriaans, J.A. Nissen and J.A. Lipa, Phys. Rev. Lett. **69** (1992) 3005;
H.B. Prosper, Am. J. Phys. **61** (1993) 54;
G.D.J. Phillies, Am. J. Phys. **52** (1984) 629.
[60] E. Schnedermann and U. Heinz, Phys. Rev. Lett. **69** (1992) 2908.
[61] P.J. Siemens and J.O. Rasumssen, Phys. Rev. Lett. **42** (1979) 880.
[62] G. Wilk and Z. Włodarczyk, Phys. Rev. Lett. **84** (2000) 2770.
[63] C.Tsallis, J. Stat. Phys. **52** (1988) 479.
[64] W.M. Alberico, A. Lavagno and P. Quarati, Eur. Phys. J. **C12** (2000) 499;
O.V. Utyuzh, G. Wilk and Z. Włodarczyk, J. Phys. **G26** (2000) L39;
I. Bediaga, E.M.F. Curado and J.M. de Miranda, Physica **A286** (2000) 156;
F.S. Navarra, O.V. Utyuzh, G. Wilk and Z. Włodarczyk, Nuovo Cim. **24C** (2001) 725;
G. Wilk and Z. Włodarczyk, Physica **A305** (2002) 227.
[65] O.V. Utyuzh, G. Wilk and Z. Włodarczyk, hep-ph/0103273.
[66] *ALICE Technical Proposal*, CERN/LHCC 95-71, LHCC/P3, Geneva, 1995, p.195.
[67] R. Korus, St. Mrówczyński, M. Rybczyński, and Z. Włodarczyk, Phys. Rev. **C64** (2001) 054908.
[68] M. Gaździcki and St. Mrówczyński, Z. Phys. C **54**, 127 (1992).
[69] C.M.G.Lates, Y.Fujimoto and S.Hasegawa, Phys.Rep. 65 (1980) 151
[70] S. Gavin et al., Phys.Rev.Lett. 72 (1994) 2143;
S. Gavin and B.Muller, Phys.Lett. B329 (1994) 486;
J. I. Kapusta and A.P.Vischer, Z.Phys. C75 (1997) 507.
[71] S. Pratt, Phys. Lett. B301 (1993) 159
[72] P.Seyboth, in Proc.XXV Int. Symposium on Multiparticle Dynamics, Stara Lesna, Slovakia, Sept.1995, D.Brancko,L.Sandor and J.Urban eds., World Scientific 1996, p.170
[73] T.C.Brooks et al., Phys.Rev. D55 (1997) 5667
[74] M.M.Aggarwal et al., Phys.Lett. B420 (1998) 169
[75] NA44 Collab.,I.Bearden et al., arXiv: nucl-ex/0107007 v1, 10 July 2001
[76] PHOS TDR, CERN/LHCC 99-4
[77] TPC TDR, CERN/LHCC 2000-01
[78] PMD TDR, CERN/LHCC 99-32
[79] K. Geiger, Phys. Rep. **258** (1995) 237.
[80] X.-N. Wang, Phys. Rep. **280** (1997) 287.
[81] N.S. Amelin et al., Phys. Rev. Lett. **67** (1991) 1523.
[82] J.-Y. Ollitrault, Phys. Rev. **D46** (1992) 229.
[83] St. Mrówczyński, Acta Phys. Pol. **B31** (2000) 2065.